A Ka-Band Fully Tunable Cavity Filter

Bahram Yassini, *Member, IEEE*, Ming Yu, *Fellow, IEEE*, and Brian Keats

Abstract—A TE_{011} Ka-band tunable filter with a stable and continuous tuning performance is presented in this paper. Both bandwidth and center-frequency tunability are demonstrated by cascading six-pole pseudo-low-pass and pseudo-high-pass tunable filters. A novel mode-splitter resonator and coupling configuration enabling cross-coupled planar TE_{011} filter realization is introduced in this paper. The concept can be applied to back-to-back coupled TE_{011} resonators as well. The filter design is verified through fabrication of multiple tunable filters that demonstrates 500 MHz of tuning range with a stable RF tuning performance.

Index Terms—Cavity resonators, coupling, reconfigurable architectures, TE_{011}, tunable filters.

I. INTRODUCTION

REALIZING a flexible transceiver, particularly for reconfigurable payloads, presents a number of technical challenges; bandwidth tunability, center-frequency tunability, and selectivity must be achieved over a wide frequency range [1]. If tunability is realized by resizing cavities, the actuation system must exhibit minimal power consumption. Latching is required to ensure that power is only consumed during a tuning operation and to maintain filter performance while the mechanism is unpowered. A key design parameter in realizing the filter function for a tunable filter is the desired mode.

The field pattern of a cylindrical cavity operating in the TE_{011} mode is an attractive choice for tunable filters. Along with a high quality factor, the field pattern and current distribution offer key advantages for realizing tunable filters. However, this mode of operation is degenerate with a pair of low-quality-factor TM_{111} modes that need to be separated from the operating TE_{011} mode without degrading the quality factor or overall filter performance [2], [3]. Realization of a filter function in a cross-coupled resonator configuration such as this presents another challenge [4]; however, a cross-coupled realization is essential since a planar layout allows for a single actuation mechanism to realize tunability. To the best of our knowledge, no demonstration of stable tuning performance using this mode can be found in the literature.

The most efficient technique to split the degenerate TM_{111} mode from the operating TE_{011} mode is shaping the cavity resonator [2], [3]. This technique uses a barrel-shaped cavity re-

lating the modes of a cylindrical cavity to those of a spherical cavity. However, this shaping method increases the overall filter footprint and is difficult to manufacture. Another technique introduced in [4] employs metallic posts to split the degenerate TM_{111} mode, but it suffers from fabrication complexity and performance degradation. In [5], a disc-loaded technique is presented for the L-band. The efficacy of this technique is not substantiated and clarified. In [5], however, the disc is not used to split the degenerate TM_{111} mode.

All of the published TE_{011} filters use a below-resonance iris (short iris) to couple two cavities. This type of iris only realizes one coupling sign in a side-to-side (planar) cross-coupled cavity configuration. Therefore, it does not offer an all-purpose and comprehensive solution to realize any desired filter function in a planar and cross-coupled fashion using TE_{011} cavity resonator.

Although the extracted-pole technique [6] can be employed to realize a filter response in a planar fashion using the same sign coupling configuration, this technique suffers from a size disadvantage. The extracted pole design is not attractive for tunable filter design because of the frequency-sensitive transmission lines used between cavities.

The back-to-back coupling employing an offset-cavity technique in two layers described in [4] can provide both positive and negative couplings. This method increases the overall filter envelope due to the offset cavity configuration. This configuration is not practical where a single actuation mechanism will simultaneously tune all cavities.

The single-layer cross-coupled cavity design presented in this paper is an attractive filter configuration, particularly for tunable filter realization. This configuration requires both positive and negative coupling to realize the desired filter function. A design that can address both coupling signs in a planar cross-coupled fashion has not been introduced in the literature. The presented tunable filter technology offers both bandwidth and center-frequency tunability. By matching the tuning curves of the cavities, a single actuation mechanism can be used for all filter cavities. This configuration minimizes power consumption and complexity.

II. END-CAP METAL-RING TM_{111} MODE-SPLITTER

In order to split the degenerate TM_{111} mode, a feature is required that will move the TM_{111} resonance, while minimally affecting the desired TE011 mode.

Electromagnetic field and current distribution for the desired TE_{011}, the degenerate TM_{111} and the high-frequency spurious TE_{311} modes are shown in Fig. 1. Normalized electric field strength versus normalized radius for all of the electric field components of these modes are also shown in Fig. 2.

TE_{011}-mode electric field strength and current distribution approach zero at both the center and edge of the cavity. Due

Mode	TE011	TM111	TE311
Electric Field (——), Magnetic Field (---) pattern			
Field component	E_φ, H_r, H_z	E_r E_φ, E_z, H_r, H_φ	E_r, E_φ H_r, H_φ, H_z
Current distribution (A/m)			
Current Scale	0 ▨▨▨▨▨▨ 1		

Fig. 1. Electric and magnetic field and current distribution for the TE_{011}, TM_{111}, and TE_{311} modes.
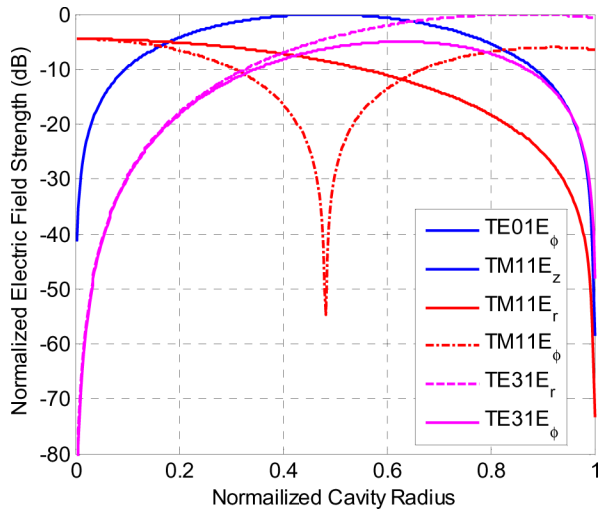

Fig. 2. Normalized electric field strength versus normalized radius.

to the weakness of the current flow and electric field at the center and edge of the end walls, introducing a properly designed perimeter channel and center bore as shown in Fig. 3 will have a minimal effect on the desired TE_{011} mode.

However, the TM_{111}-mode current distribution is strong at both the center and edge of the end wall. Both radial and angular components of the electric field are strong at the center while the radial component is also strong at the perimeter. Although the longitudinal component of this mode (E_z) follows the same distribution versus cavity radius as the angular component of the TE_{011} electric field, it has the opposite distribution along resonator axis and has its maximum at the end wall. The perimeter channel and center bore described in Fig. 3 will therefore perturb this mode strongly and lower the resonant frequency significantly. The magnitude of this shift depends on the dimensions of the channel and bore. The bore diameter should be less than 48% of cavity diameter since longitudinal electric field of TM_{111} is maximum at this point, and the bore will counter-affect the gap if it is larger than that value.

The high-frequency spurious TE_{311} mode is strong at the end-wall edge and weak at the center. Its resonant frequency

is also shifted lower by the end cap channel and bore. However, the impact is significantly less than on the TM_{111} mode due to the longitudinal electric component of the TM_{111} mode being maximum at the end cap. The impact is also lessened by the differing field and current distribution (Fig. 1).

The channel and bore dimensions should be carefully designed to optimize the spurious-free window with the minimum impact on the TE_{011} quality factor or exciting other unwanted modes.

The structural details of the mode-splitting end cap are shown in Fig. 3. The combination of the perimeter channel and center bore forms an end-cap metal ring mode-splitter.

The cavity can be loaded with one or two mode-splitters, depending on the application. The channel can cause unwanted resonance if the length is too close to a quarter-wavelength (of free space). The channel length must therefore be well below a quarter wavelength to avoid these unwanted resonant frequencies.

A movable end cap can be introduced in the cavity to make it tunable, as shown in the Fig. 3. Electrical contact must be provided between the end of the channel and the cavity wall. The enclosure contact must provide adequate conductivity to create a near short-circuit condition. This will guarantee that the degenerate TM_{111} mode and other spurious modes are kept outside of the operating frequency range. This criterion can also be achieved with reactive impedance. Violating this condition may provide unwanted surface impedance that will not only shift the TE_{311} and TM_{111} mode undesirably, but also create other unwanted resonant modes that can be sufficiently close to the operating frequency to degrade the overall filter performance.

It is well known that the imperfect conductivity at the enclosure contact does not affect the quality factor of the operating TE_{011} mode. Therefore, the enclosure criteria can be met with a sliding contact mechanism to create tunability for a resonator or filter.

The spurious performance of the proposed resonator is shown in Fig. 4. A resonator without the center bore is shown for comparison. The channel length is varied from 0.05 to 0.09 in and TE_{011}, TM_{11}, and TE_{311} resonant frequencies are computed using a full-wave solver. More than 2 GHz of spurious-free window (TE_{311}-TM_{11}) is achieved using this technique. The figure shows that the center bore shifts the degenerate TM_{111} mode further toward lower frequencies without impacting TE_{011} and TE_{311} modes. For the dimensions shown here, end caps with both a perimeter channel and center bore increase the spurious-free window by 400 MHz compared with a perimeter channel alone.

III. LONG IRIS FOR POSITIVE COUPLING

A coupled TE_{011} resonator is shown in Fig. 5. Coupling is realized through an iris. It is common practice to use an iris with a length less than half the free-space wavelength (below resonance). This type of iris is referred to here as a *short iris*. A short iris provides only negative coupling.

Introducing an iris with positive coupling offers additional design flexibility, since it allows for a filter layout with both
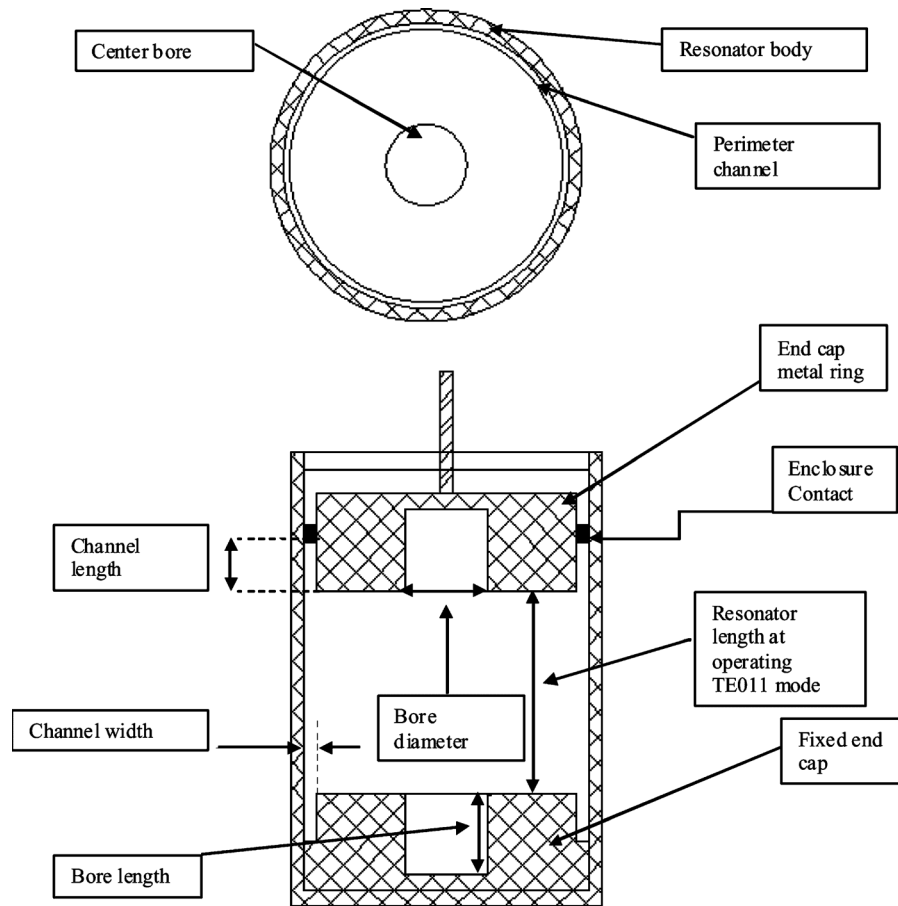
Fig. 3.   Tunable TE_{011} resonator with mode-splitter rings.

coupling signs. An iris with a length longer than half of the free-space wavelength (over the resonance) can provide positive coupling (opposite sign of the short iris) between cavities. This configuration is referred to here as a *long iris*. The following is an example on how these two irises are different.

Table I shows the simulated odd- and even-mode frequencies for short and long irises in a side-to-side metal ring loaded TE_{011} coupled resonators. It has to be noted that cavities should be properly sized to fit the long iris without performance degradation. It is clear from this table that the coupling sign of the long iris is opposite of the one for the short iris. The idea of the long iris is also applicable to the back-to-back coupled resonator.

One interesting characteristic of the long iris is its low sensitivity to its height variation and to the cavity length (cavity resonant frequency) change. This feature makes it a good candidate for applications that require stable coupling over a wide frequency range or cavity-length variation. Consider a block of two coupled side-by-side TE_{011} tunable resonator, as shown in Fig. 5. The top end walls of both cavities include metal rings displaced by ± 0.02 in to represent more than 450-MHz range at Ka-band (20 GHz). Coupling variation for short and long irises is shown in Fig. 6. This figure shows that the long iris coupling value variation is less than 3.5% versus 10% for the short iris over more than 450 MHz (around 2.5%) of tuning range. Therefore, tunable filters with a stable response can be designed by incorporating long irises in the design.

IV. APPLICATION IN FILTER DESIGN

The introduction of a long iris offering positive coupling (along with a short iris with negative coupling) can be employed to improve the TE011 filter design for both functionality and layout. Realizing many filter functions in a cross-coupled planar TE011 structure is feasible by employing long and short irises properly.

A. A Four-Pole Elliptic Filter Function

Both coupling signs are required to realize a cross-coupled four-pole elliptical filter function with two transmission zeros. Long and short irises can be used to realize such a filter in a planar TE011 configuration, as shown in Fig. 7. The filter structure comprises of three sequentially coupled long irises (positive signs) and one short iris to realize negative cross coupling. Resonators are loaded metal-ring mode splitters to isolate the TM_{111} mode. Input and output ports are rotated by 30° to minimize stray coupling and balance the notches. Full-wave simulation of such a filter is shown in Fig. 8. The in-band response is clean, and the degenerate mode is shifted down as expected. Simulation demonstrates that the degenerate TM_{111} mode is lowered by another 450 MHz by the center bore as expected.

B. Realizing Planar Asymmetric Filter Functions

Asymmetric filter functions can be realized using trisection building blocks as shown in Fig. 9. Trisection building blocks
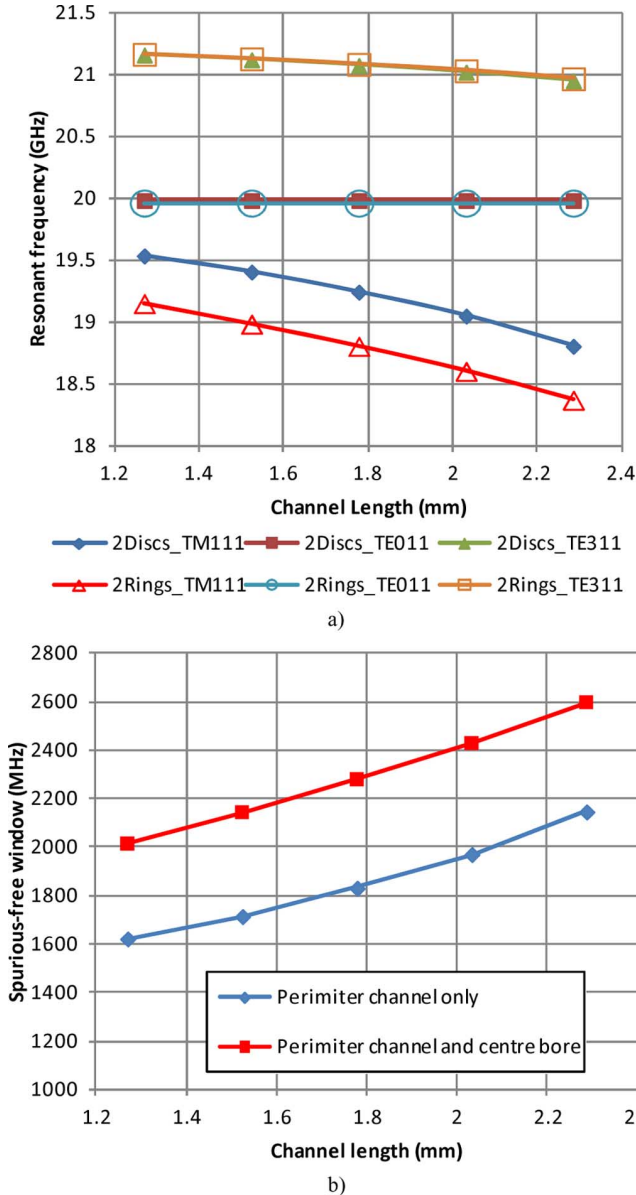
a)

b)

Fig. 4. Spurious modes for a 20-GHz TE_{011} resonator with metal ring mode-splitter. Channel width = 0.51 mm, bore diameter = 6.35 mm, cavity diameter = 22.23 mm, and resonator length = 13.18 mm. (a) TE_{011} and the closest spurious modes. (b) Spurious-free window.
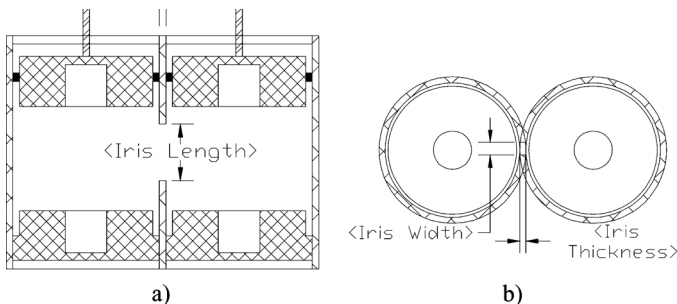

Fig. 5. Two TE_{011} metal ring-loaded resonators coupled through an iris. (a) Side view. (b) Top view.

offer size and expandability advantages. Coupling structure for both pseudo-low-pass and pseudo-high-pass 6-2 filters are

TABLE I
BOTH COUPLING SIGNS FOR A DIRECT COUPLED TE_{011} CAVITIES

	Short Iris	Long Iris
Freq (GHz)	20	20
Cavity length (mm)	13.18	13.18
Free space λ/2 (mm)	~7.49	~7.49
Iris Length (mm)	5.08	10.16
Iris width (mm)	3.81	3.81
f_{odd} (GHz)	19.808	20.093
f_{even} (GHz)	19.913	19.88
Coupling sign	Negative ($f_{odd} < f_{even}$)	Positive ($f_{odd} > f_{even}$)

shown in Fig. 9(a) and (b), respectively. These are six-pole filters with two transmission zeros. Each trisection provides three poles and one transmission zero.
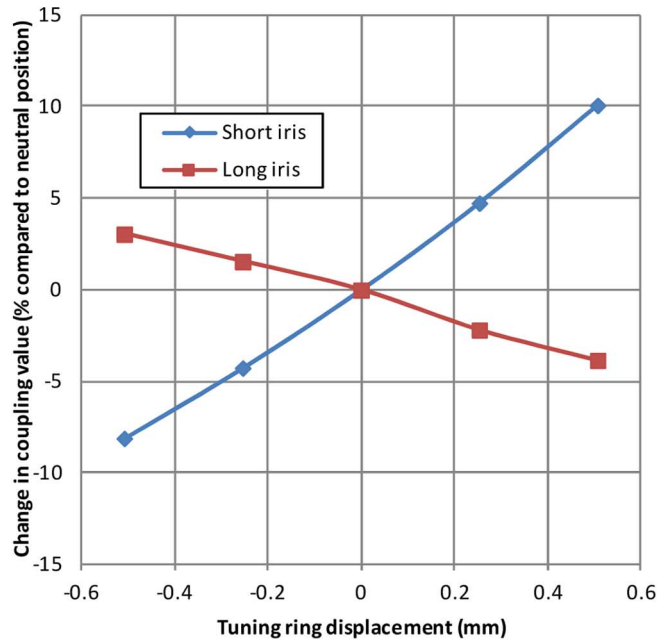
Although both pseudo-low-pass and pseudo-high-pass coupling matrices are not unique, one can conclude that the pseudo-low-pass version is not realizable without positive coupling [7]. The positive-coupling long iris is used to realize this filter. A cross-coupled pseudo-low-pass filter employing all positive coupling signs is shown in Fig. 9(a). This filter function is realizable in a planar TE_{011} direct-coupled configuration using the introduced long iris [8]. Fig. 10 shows a layout of such a filter incorporating two trisections and cavities loaded with a metal-ring mode splitter. All of the TE_{011} resonator cavities are directly coupled using long irises to realize positive coupling. The same layout with different iris sizes can be used for pseudo-high-pass versions to realize the coupling structure shown in Fig. 9(b). A pseudo-high-pass filter is also realizable using all negative coupling signs.
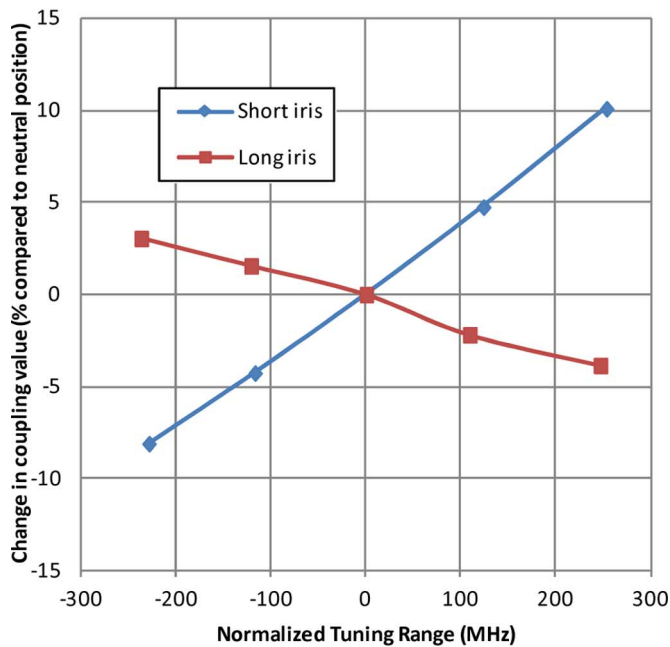
V. TUNABLE TE_{011} FILTER

A variety of tunable filter technologies have been reported in literature and industry [9]–[21]. Presenting both bandwidth and center frequency tunability with a stable response over a wide tuning range is still a major challenge among them. It is known that bandwidth adjustment can be realized by cascading two (low-pass and high-pass) tunable filters. Both bandwidth and center frequency can then be tuned by tuning each filter center frequency with respect to each other. The resultant cascaded performance is the overlap of the two filter responses.

Both filters should maintain their in-band and rejection performance when tuning center frequency. This is the main challenge in the cascade approach, particularly at microwave frequencies. The introduced tunable metal-ring loaded TE_{011} cavity and long coupling iris (positive coupling) are the key elements to realize such a stable tunable filter response.

TE_{011} metal-ring loaded cavity resonators and combinations of long and short irises can be employed to realize both pseudo-low-pass and pseudo-high-pass filters in the same planar layout, as shown in Fig. 10. The center bore of the metal ring is not used for simplicity in the example provided in this paper. The center bore can be added if a wider spurious-free window is required.

Fig. 7. Four-pole planar TE_{011} filter incorporating mode-splitter ring and long and short irises to realize elliptic filter function.

Fig. 6. Coupling value variation for a Ka-band (20 GHz) metal ring-loaded TE_{011} coupled resonators. (a) Coupling variation versus displacement (b) Coupling variation versus resonance frequency.

It is important where possible to use (long) positive coupling irises in both designs to achieve a stable RF performance over the tuning range as the long iris exhibits a very small coupling variation over the tuning range (Fig. 6). Therefore, the pseudo-low-pass filter is realized using all positive (long) coupling irises. The pseudo-high-pass version is realized using five positive (long) coupling irises for sequential coupling and two negative (short) coupling irises for cross coupling. Input and output irises are located at 90° with respect to the sequential
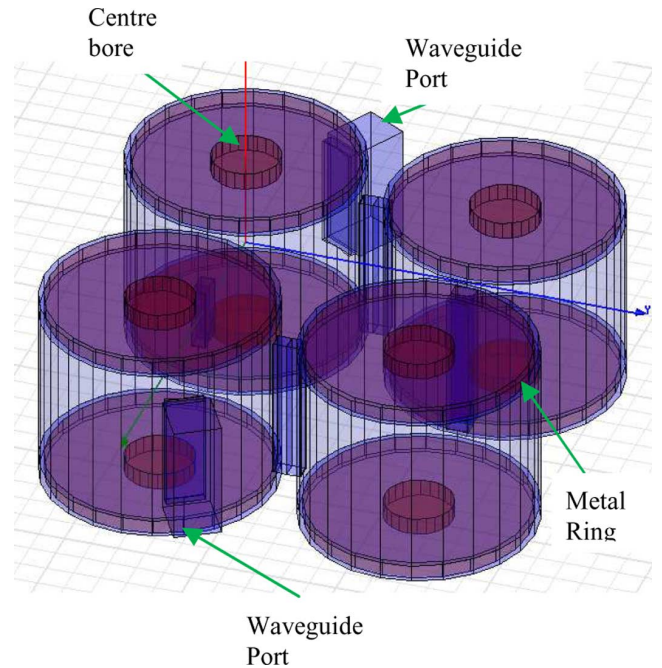
coupling irises (Iris-12 and Iris-56, respectively) to suppress TE_{311} coupling and reduce stray coupling.

Each cavity has a different resonant frequency, as shown by coupling matrices in Fig. 9(a) and (b). Therefore, tuning curves of cavities must match each other to maintain filter response over the tuning range. Independent cavity actuation can achieve that at the cost of multiple actuation systems and a more complex tuning mechanism. A single actuation mechanism is possible if the tuning curves are matched for each cavity.

The resonant frequency of each TE_{011} cavity is governed by the following equation:

$$f_i = A\sqrt{\left(\frac{\chi'_{01}}{r_i}\right)^2 + \left(\frac{\pi}{l_i}\right)^2}$$
$$A = \frac{1}{2\pi\sqrt{\mu\varepsilon}} \quad (1)$$

where χ'_{01} is the first zero of the derivative of the Bessel function of the first kind and order 0 and l_i and r_i are length and radius of the ith cavity, respectively.

The derivative of resonant frequency of each cavity with respect to its length can be derived from (1) as

$$\frac{\partial f_i}{\partial l_i} = -(A\pi)^2 \frac{1}{f_i l_i^3}. \quad (2)$$

Therefore, the following criterion ensures that resonator tuning curves matches at the middle of the tuning range:

$$f_i l_i^3 = f_j l_j^3. \quad (3)$$

Considering the typical dimensions of a Ka-band (20 GHz) TE_{011} filter (Fig. 4) and (2), the tuning slope is in the range of
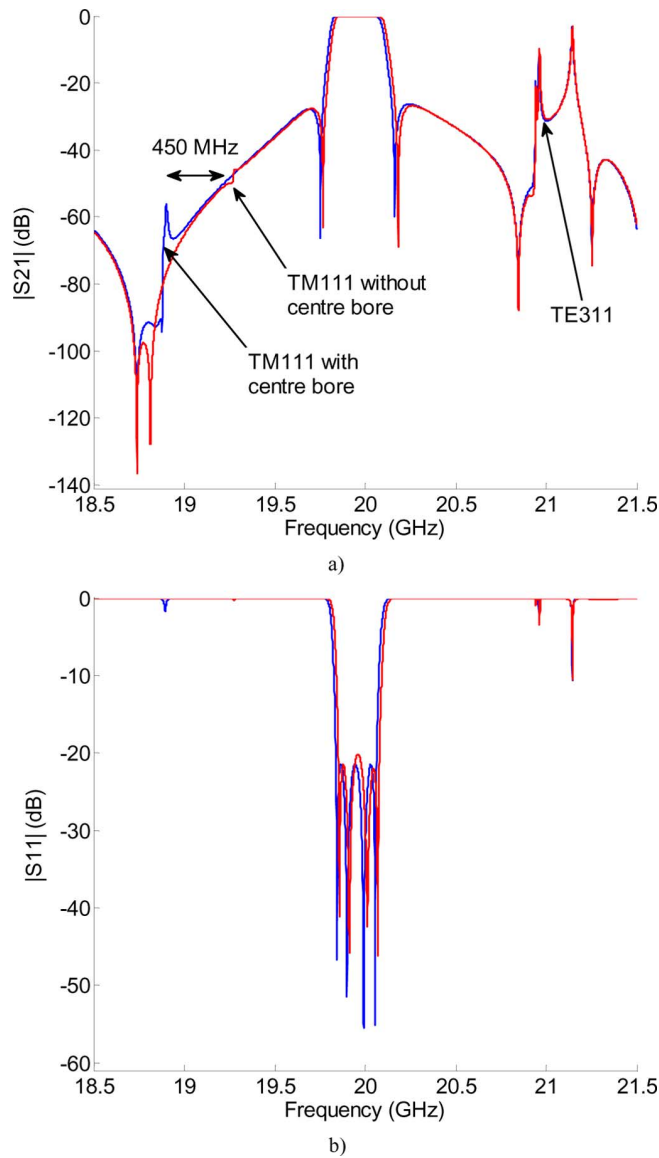
Fig. 8. Simulated response of a four-pole planar TE_{011} elliptic filter. The design with (blue) and without (red) center bore shows that the center bore helps to further split the TM_{111} mode by 450 MHz without affecting TE_{311} spurious. (a) Transmission response. (b) Return loss.
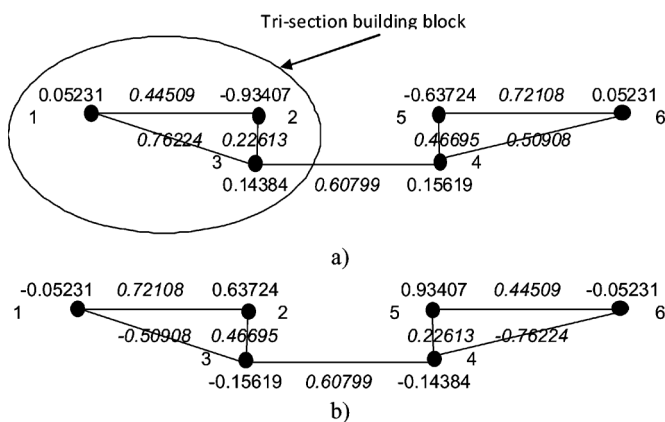

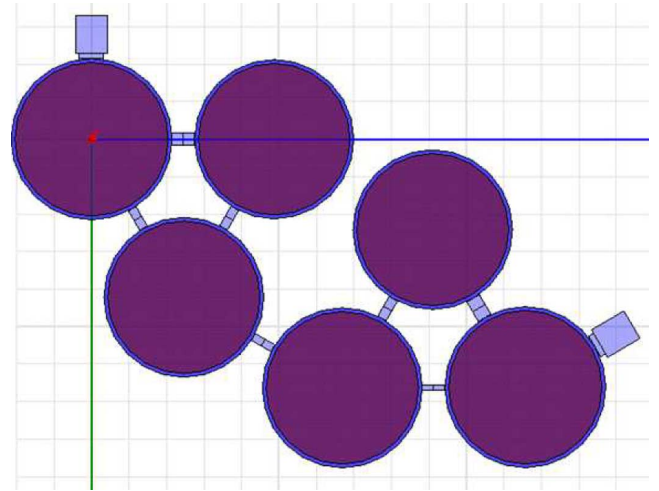Fig. 9. Coupling matrix for (a) pseudo-low-pass and (b) pseudo-high-pass six-pole filter.

Fig. 10. Cross-coupled planar TE_{011} filter layout incorporating metal-ring mode-splitter and long/short irises to realize both pseudo-low-pass and pseudo-high-pass 6-2 filter functions.
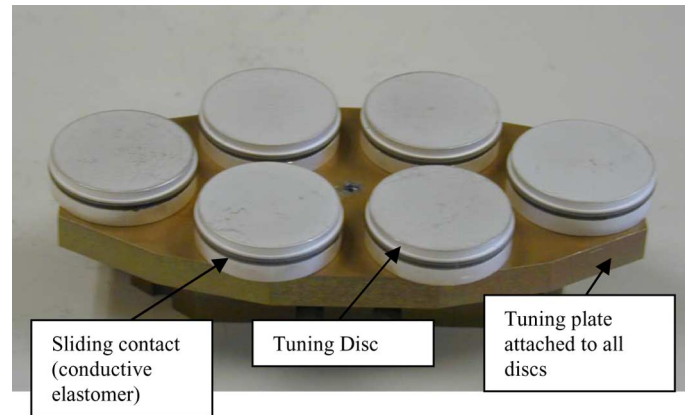

Fig. 11. Tunable filter moving section including tuning plate, tuning disc/plunger, and sliding contact.

10 MHz/mil. Thus, ± 25 mil ($\pm 5\%$ of cavity length) is required for ± 250-MHz (a total of 500 MHz) tuning range. Bearing in mind the self-coupling values presented in the coupling structure from Fig. 9, a bandwidth of 170 MHz, and a tuning range of 500 MHz, one can use the first-order approximation of (3) and derive the following formula for the length of each cavity with respect to the length of first resonator or any desired reference resonator:

$$l_i = l_1 \left(1 - \frac{f_i - f_1}{3 f_1} \right). \tag{4}$$

Criterion (4) is satisfied by properly choosing each cavity diameter at the middle of the tuning range. Therefore, a uniform plunger displacement incorporating single actuation is adequate to provide an efficient and cost-effective tuning mechanism.

The moving part of the tunable filter including tuning plate and six plungers is shown in Fig. 11. Each plunger contains a mode-splitter disc and a sliding contact, as shown in Fig. 11. A conductive elastomer tube is used to provide sliding contact.
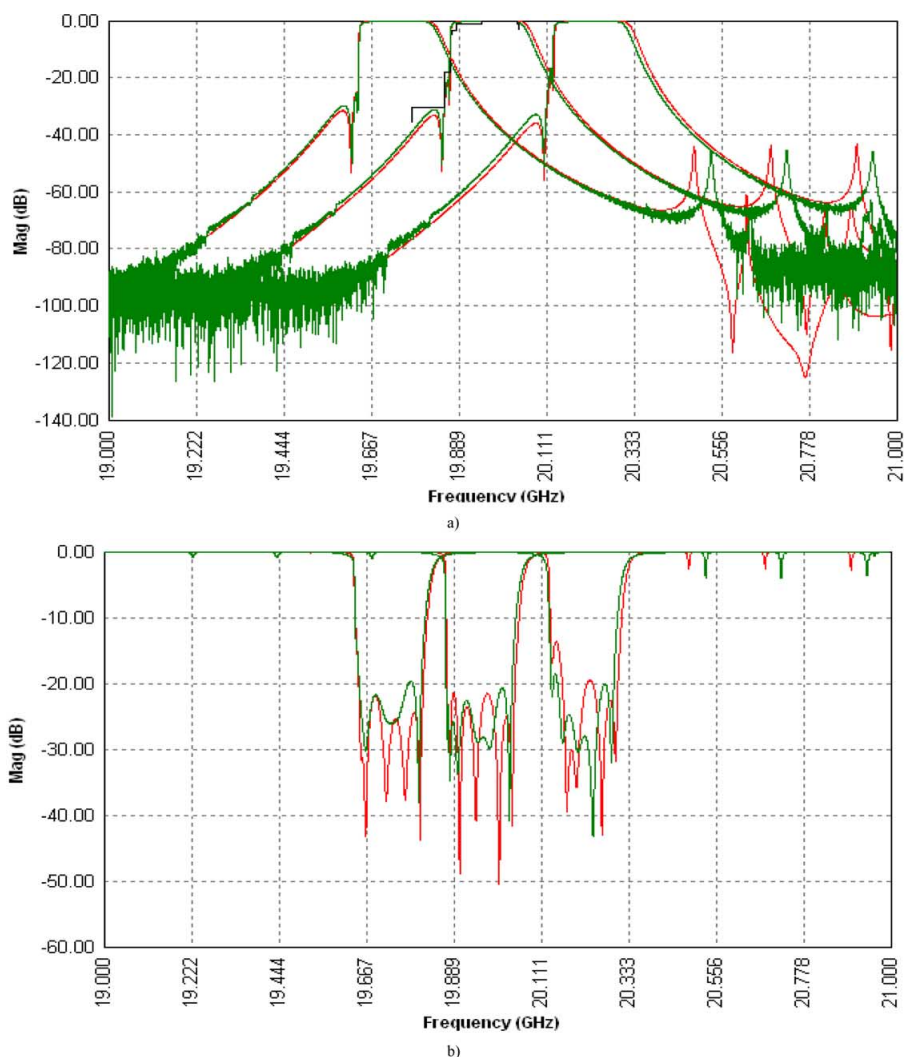
Fig. 12.   Tunable filter performance over 500-MHz range. (a) Pseudo-high-pass tunable filter transmission response ($|S21|$). Simulation in (red) and measurement (green). (b) Pseudo-high-pass tunable filter return loss ($|S11|$). Simulation in (red) and measurement (green).

The elastomer has a conductivity of 20 000 S/m, providing adequate conductivity to enclose other modes (particularly TM_{111} and TE_{311}). The sliding contact does not affect the TE_{011} mode as was described in the previous section.

The filter is tuned over the desired tuning range by adjusting the tuning plate attached to the six plungers using a stepper motor. RF tuning performance of both TE_{011} tunable pseudo-high-pass and pseudo-low-pass filters are shown in Fig. 12. Fig. 12(a) and (b) includes simulated performance for comparison. The in-band performance is clean and the degenerate TM_{11} mode is moved lower as expected.

A 500-MHz tuning range is demonstrated through ±0.0027-in adjustment of the tuning plate using a stepper motor. Stable tuning performance is achieved. Nominal 3-dB bandwidth at the center of tuning range is 190 and 200 MHz for pseudo-high-pass and pseudo-low-pass filters, respectively. Bandwidth variation is less than 1.5% (±3 MHz) for both tunable filters over the 500-MHz tuning range. Both filter shapes are stable over the entire 2.5% tuning range. Return loss is maintained at better than 17 and 20 dB for pseudo-high-pass

and pseudo-low-pass tunable filters, respectively. To the best of our knowledge, this is the best tuning performance demonstrated in the literature.

Near-band rejection performance is stable, particularly for the pseudo-low-pass version where the filter exhibits stable notch levels over the entire measured tuning range. Overall tuning performance for the pseudo-low-pass version is more stable since it uses only long irises for coupling.

Measured minimum insertion loss and extracted Q maintained their value between 0.2–0.22 dB and 15 500–16 000 over the 500-MHz tuning range. The simulated values for insertion loss and Q are 0.16–0.17 dB and 18 000. Comparing simulated and measured values verifies that the sliding contact is not degrading filter performance. The presented technology has a great advantage over microelectromechanical systems (MEMS) and varactor-based technologies and techniques since it can handle high power and has a potential application for output circuits [22], [23].

Fabricated pseudo-low-pass and pseudo-high-pass tunable filters are used in a cascade configuration, as shown in Figs. 13
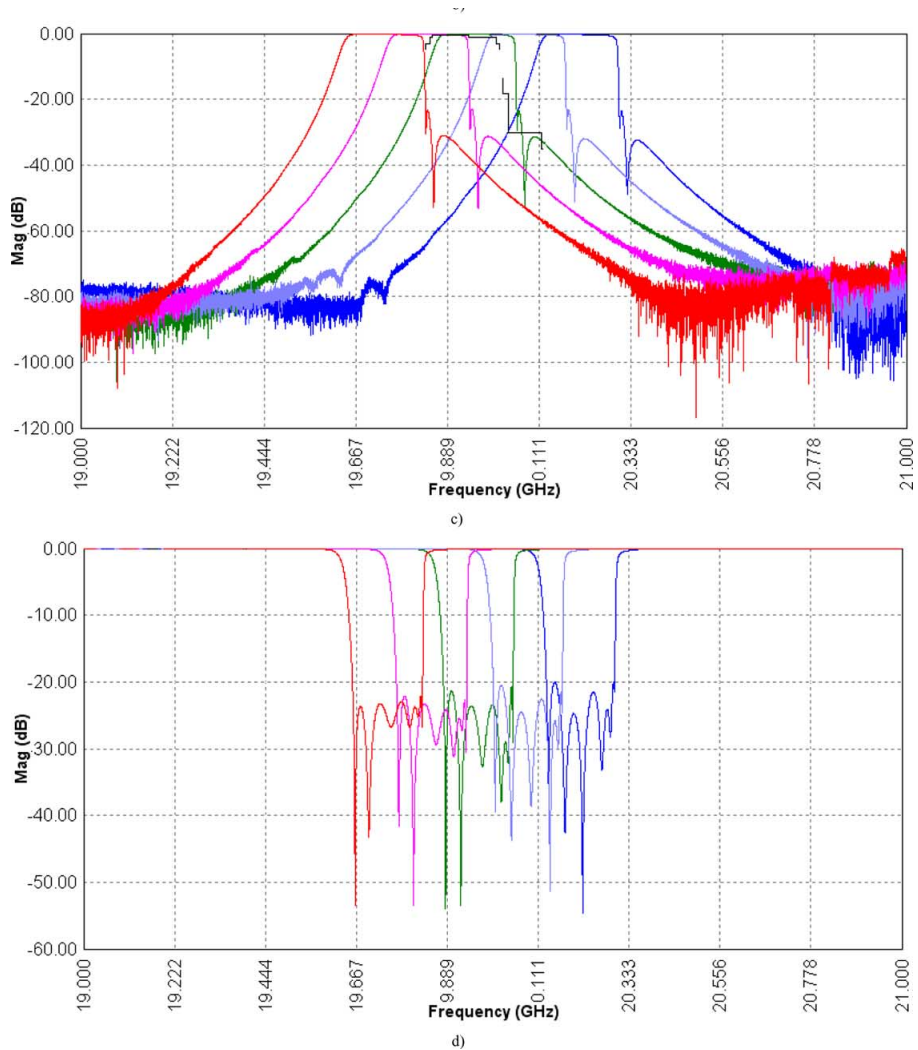
Fig. 12. *(Continued.)* Tunable filter performance over 500-MHz range. (c) Pseudo-low-pass tunable filter transmission response ($|S21|$). (d) Pseudo-low-pass tunable filter return loss ($|S11|$).
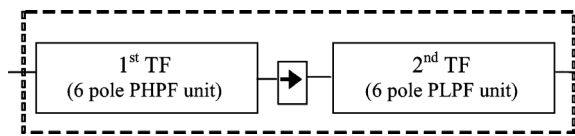

Fig. 13. Tunable filter block diagram in a cascade configuration capable of tuning center frequency and bandwidth.

Fig. 14. Cascaded TE_{011} tunable pseudo-low-pass and psuedo-high-pass filters to realize full tunable filter with center frequency and bandwidth tenability.

and 14, to realize both bandwidth and center frequency tunability. An isolator is used to connect the two halves of the tunable filter as shown in Fig. 14. Measured tuning performance is shown in Fig. 15. A bandwidth tuning of 40–160 MHz over more than 500-MHz tuning range is exhibited maintaining a very stable in-band and out-of-band performance.

The realized tunable filter achieves a step size of 1 MHz. The repeatability of the mechanism was demonstrated over a life test that consisted of 1400 iterations across the 500-MHz tuning range in 125-MHz increments for a total of 11 201 actuations. The total worst case variation of the -3-dB band-edge measured during this test was 0.94 MHz (Fig. 16).
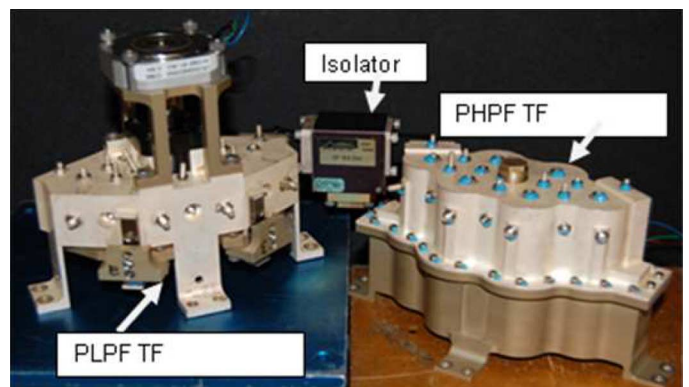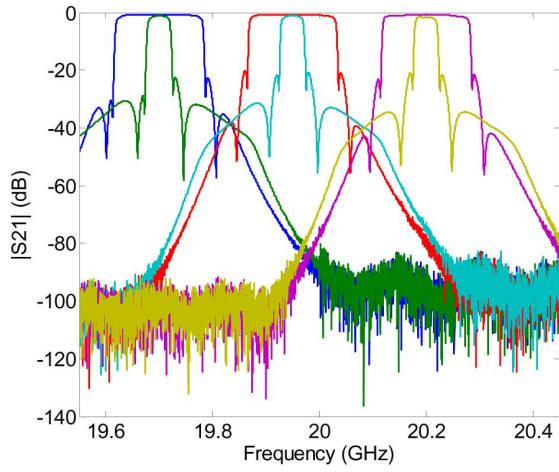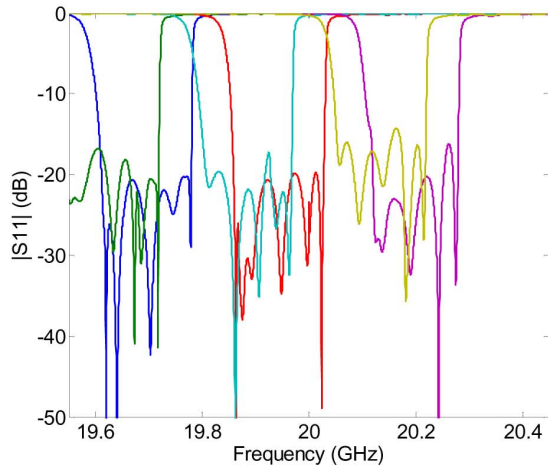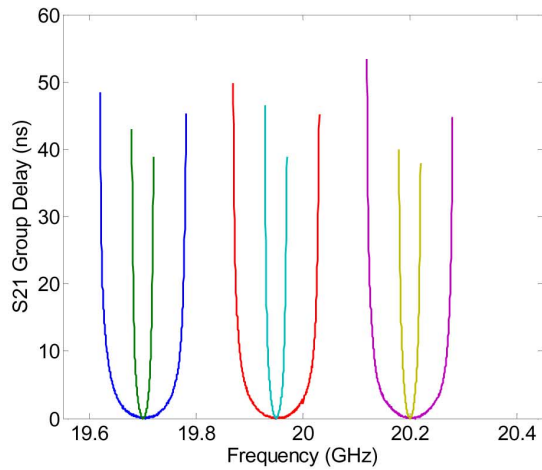
The precision of the fine-tuning performance is shown across the tuning range (single-step) in Fig. 17. A frequency lookup-table (LUT) was constructed from prior measured tuning performance. The measured error with respect to the LUT is shown,

Fig. 15. Tunable filter measured performance. Shown is 40–160-MHz bandwidth tuning over more than 500 MHz of center frequency tuning range with a very stable performance. (a) Cascaded filter transmission response. (b) Cascaded filter input return loss. (c) Cascaded filter group delay (normalized, within −3-dB bandwidth).

Fig. 16. Measured −3-dB band edge over 11 201 actuations.
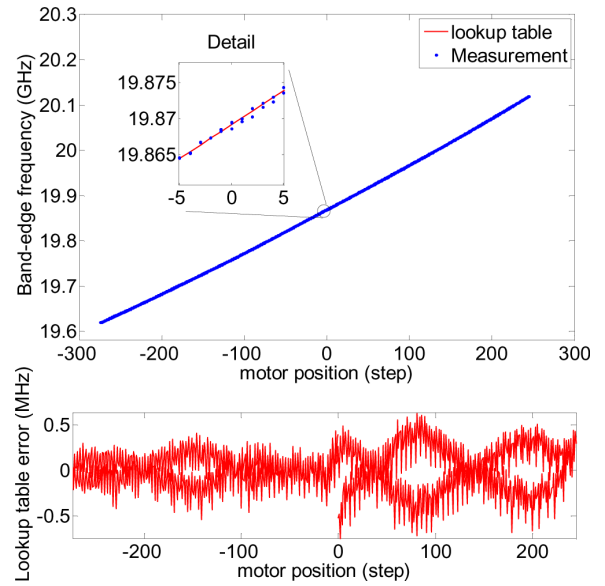
Fig. 17. Measured tuning precision.
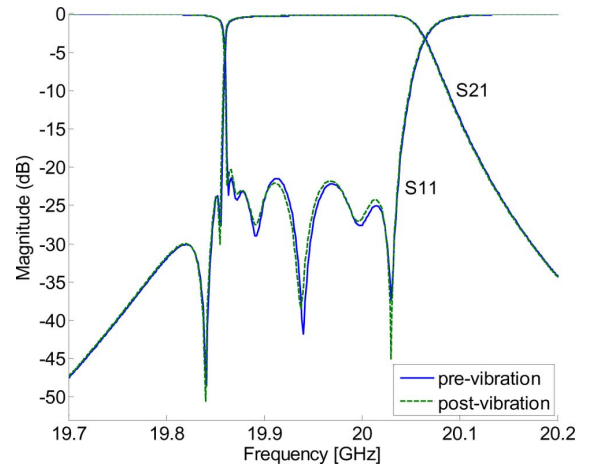
Fig. 18. Measured pseudo-high-pass filter response pre- and post-vibration.

along with the measured −3-dB band edge. The LUT error is within approximately ±0.5 MHz.

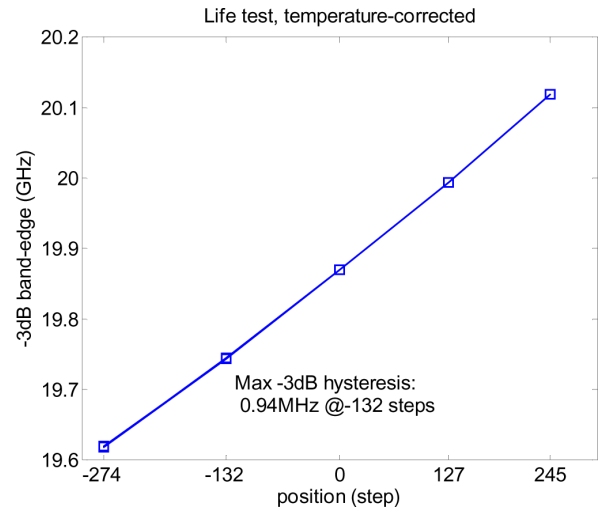The pseudo-high-pass filter was subjected to random vibration of 12.8 G_{rms} in the planar axes and 21.4 G_{rms} in the out-of-plane axis. The pre- and post-vibration filter response is shown in Fig. 18. The filter response is unaffected by dynamic loading.

The details of the mechanism design are beyond the scope of this paper. These data are presented to demonstrate that this filter design can be realized with a robust tuning mechanism capable of achieving excellent tuning resolution and repeatability, while simultaneously withstanding dynamic loads typical of space applications.

VI. CONCLUSION

A metal-ring loaded TE_{011} resonator is shown to offer wide spurious-free window by splitting the degenerate TM_{111} mode. The introduced resonator offers tunability without performance degradation.

A cross-coupled planar TE_{011} cavity resonator incorporating an end-cap metal ring feature and a novel long iris to realize positive coupling in a direct-coupled cavity layout is introduced in this paper. The long iris allows for any transmission zero locations to be realized in a cross-coupled planar TE_{011} configuration.

Pseudo-low-pass and pseudo-high-pass tunable filters with complex filter function and stable tuning performance were designed and fabricated using the presented idea. Both filters employ the same layout and actuation mechanism. To the best of our knowledge, this is the most stable tunable filter presented in the literature with respect to return loss and transmission zeros. The filter maintains steep selectivity and excellent return loss over the tuning range.

A 40–160-MHz bandwidth and 500-MHz center frequency tuning range at the 20-GHz band was exhibited by cascading pseudo-low-pass and pseudo-high-pass tunable filters.

The tuning mechanism exhibits a resolution of 1 MHz and a repeatability of 0.94 MHz over an 11 201 actuation life test. The measured tuning error is approximately ±0.5 MHz with respect to an LUT. The pseudo-high-pass filter response is maintained after vibration testing.

ACKNOWLEDGMENT

The authors would like to thank J. Cox, D. Smith, and V. Dokas for performing assembly, tuning, and measurement and S. Choi and K. Engel for providing valuable practical comments and inputs for fabrication.

REFERENCES

[1] W. Graham, T. Glyn, C. Gary, and M. Ian, "Agile equipments for an advanced Ku/Ka satellite," in *Proc. 24th AIAA Int. Commun. Satellite Syst. Conf.*, San Diego, CA, Jun. 14, 2006, Art. ID AIAA 2006-5396.

[2] "Biconical Multimode Resonator," U.S. Patent 5 614 877.

[3] H. L. Thal, Jr, "Cylindrical TE011/TM111 mode control by cavity shaping," in *IEEE Transactions on Microwave Theory and Techniques*, New York, Dec. 1979, vol. 27, pp. 982–986.

[4] A. E. Atia and A. E. Williams, "General TE011-mode waveguide band-pass filters," *IEEE Trans. Microw. Theory Tech.*, vol. MTT-24, no. 10, pp. 640–640, Oct. 1976.

[5] G. L. Matthaei, L. Young, and E. M. T. Jones, *Microwave Filters, Impedance-matching Networks, and Coupling Structures*. New York: McGraw-Hill, 1964, pp. 921–934.

[6] R. J. Cameron, H. G. Grecg, C. J. Radcliffe, and J. D. Rhodes, "Extracted-pole filter manifold multiplexing," *IEEE Trans. Microw. Theory Tech.*, vol. MTT-30, no. 7, pp. 1041–1050, Jul. 1982.

[7] R. J. Cameron, C. M. Kudsia, and R. R. Mansour, *Microwave Filters for Communication Systems*. Upper Saddle River, NJ: Wiley, 2007.

[8] Y. Bahram, Y. Ming, and K. Brian, "A *Ka*-band planar TE011 mode cavity tunable filter using a mode-splitter ring," in *IEEE MTT-S Int. Microw. Symp. Dig.*, Jun. 17–22, 2012, pp. 1–3.

[9] B. Yassini, M. Yu, and S. Kellett, "A *Ku*-band high-Q tunable filter with stable tuning response," *IEEE Trans. Microw. Theory Tech.*, vol. 57, no. 12, pp. 2948–2957, Dec. 2009.

[10] W. Da-Peng, C. Wen-Quan, and P. Russer, "Tunable substrate-integrated waveguide (SIW) dual-mode square cavity filter with metal cylinders," in *Proc. IEEE MTT-S Int. Microw. Workshop Series on Art of Miniaturizing RF and Microwave Passive Components*, 2008, pp. 128–131.

[11] V. E. Boria, M. Guglielmi, and P. Arcioni, "Computer-aided design of inductively coupled rectangular waveguide filters including tuning elements," *Int. J. RF Microw. Comput.-Aided Eng.*, vol. 8, no. 3, pp. 226–235, May 1998.

[12] T. P. Vuong, G. Fontgalland, R. Crampagne, H. Baudrand, and C. Zanchi, "Tuneable irises for rectangular waveguide filter microwave conference," in *Proc. 30th Eur. Microw. Conf.*, 2000, pp. 1–4.

[13] R. Lech, A. Kusiek, and J. Mazur, "Tuning properties of irregular posts in waveguide junctions—Tunable filter application," in *Proc. 18th Int. Conf. Microw. Radar and Wireless Commun.*, 2010, pp. 1–4.

[14] V. Boria and B. Gimeno, "Waveguide filters for satellites," *IEEE Microw. Mag.*, vol. 8, no. 10, pp. 60–70, Oct. 2007.

[15] E. Pistono, M. Robert, L. Duvillaret, J. Duchamp, A. Vilcot, and P. Ferrari, "Compact fixed and tune-all bandpass filters based on coupled slow-wave resonators," *IEEE Trans. Microw. Theory Tech.*, vol. 54, no. 6, pp. 2790–2799, Jun. 2006.

[16] Y. Liu, A. Borgioli, A. S. Nagra, and R. A. York, "Distributed MEMS transmission lines for tunable filter applications," *Int. J. RF Microw. Comput.-Aided Eng.*, vol. 11, no. 5, pp. 254–260, Sep. 2001.

[17] A. Abbaspour-Tamijani, L. Dussopt, and G. M. Rebeiz, "A millimeter-wave tunable filter using MEMS capacitors," in *Proc. 32nd Eur. Microw. Conf.*, Milan, Italy, Sep. 2002, pp. 813–815.

[18] D. Mercier, J.-C. Orlianges, T. Delage, C. Champeaux, A. Catherinot, D. Cros, and P. Blondy, "Millimeter-wave tune-all bandpass filters," *IEEE Trans. Microw. Theory Tech.*, vol. 52, no. 4, pp. 1175–1181, Apr. 2004.

[19] J. Uher and W. J. R. Hoefer, "Tunable microwave and millimeter-wave band-pass filters," *IEEE Trans. Microw. Theory Tech*, vol. 39, no. 4, pp. 643–653, Apr. 1991.

[20] S. Toyoda, "Variable bandpass filters using varactor diodes," *IEEE Trans. Microw. Theory Tech*, vol. MTT-29, no. 4, pp. 363–363, Apr. 1981.

[21] A. P. Benguerel and N. S. Nahman, "A varactor tuned UHF coaxial filter," *IEEE Trans. Microw. Theory Tech*, vol. MTT-12, no. 4, pp. 468–469, Jul. 1964.

[22] S. Lundquist, M. Yu, D. J. Smith, and W. Fitzpatrick, "Application of high power output multiplexers for communication satellites," in *Proc. 20th AIAA Int. Commun. Satellite Syst. Conf. Exhibit*, May 12–15, 2002, paper 2002-1992.

[23] M. Yu, "Power-handling capability for RF filters," *IEEE Microw. Mag.*, vol. 8, no. 5, pp. 88–97, Oct. 2007.

Bahram Yassini (S'89–M'02) received the M.A.Sc. degree in electrical engineering from the University of Waterloo, Waterloo, ON, Canada, in 2001.

In 2001, he joined COM DEV Ltd., Cambridge, ON, Canada, where he is currently a Principal Member of Technical Staff in the R&D Department. His work includes design, analysis, and modeling of RF/microwave hardware, microelectromechanical systems switches, low-temperature cofired ceramic interconnects, and low-noise amplifiers for ground and space applications. Prior to that, he was with Algorex Canada, where he was involved with RF/wireless channel modeling as an RF Engineer, Italtel SPA, where he was involved with digital radio networks as a Senior Technical Advisor, and MATN, where he was involved with wireless and satellite communication systems as a Senior Radio System Engineer.

Ming Yu (S'90–M'93–SM'01–F'09) received the Ph.D. degree in electrical engineering from the University of Victoria, Victoria, BC, Canada, in 1995.

In 1993, while working on his doctoral dissertation part-time, he joined COM DEV Ltd., Cambridge, ON, Canada, as a Member of Technical Staff. He was involved in designing passive microwave/RF hardware from 300 MHz to 60 GHz for both space- and ground-based applications. He was also a principal developer of a variety of COM DEV's core design and tuning software for microwave filters and multiplexers, including computer aide tuning software in 1994 and fully automated robotic diplexer tuning system in 1999. His varied experience also includes being the Manager of Filter/Multiplexer Technology (Space Group) and Staff Scientist of Corporate Research and Development (R&D). He is currently the Chief Scientist and Director of the R&D Department, COM DEV Ltd., where he is responsible for overseeing the development of company R&D Roadmap and next-generation products and technologies, including high-frequency and high-power engineering, electromagnetic-based computer-aided design and tuning for complex and large problems, and novel miniaturization techniques for microwave networks. He is also an Adjunct Professor with the University of Waterloo, ON, Canada. He holds NSERC Discovery Grant from 2004 to 2015 with the University of Waterloo. He has authored or coauthored over 100 publications and numerous proprietary reports. He holds eight patents with six more pending.

Dr. Yu is an IEEE Distinguished Microwave Lecturer from 2010 to 2012. He has been the IEEE Microwave Theory and Techniques Society (MTT-S) Filter committee Chair (MTT-8) since 2010 and served as Chair of TPC-11. He is an associate editor of the IEEE TRANSACTIONS ON MICROWAVE THEORY AND TECHNIQUES. He was the recipient of the 1995 and 2006 COM DEV Achievement Award for the development a computer-aided tuning algorithms and systems for microwave filters and multiplexers.

Brian F. Keats received the B.A.Sc. degree in mechanical engineering, M.A.Sc. degree in electrical and computer engineering, and Ph.D. degree from the University of Waterloo, Waterloo, ON, Canada, in 2001. 2003, and 2007, respectively.

Upon completion of his studies, he joined COM DEV Ltd., Cambridge, ON, Canada, as a Post-Doctoral Fellow, where he has been involved in the design, development, and testing of a variety of products including temperature-compensated filters, tunable filters, and RF switches. He is currently a Senior Member of the Technical Staff with the R&D Department and an Adjunct Lecturer at the University of Waterloo, Waterloo, ON, Canada.